A Family of Low-Molecular-Weight Hydrogelators Based on L-Lysine Derivatives with a Positively Charged Terminal Group

Masahiro Suzuki,*[a] Mariko Yumoto,[b] Mutsumi Kimura,[b] Hirofusa Shirai,[b] and Kenji Hanabusa[a]

Abstract: A family of L-lysine-based low-molecular-weight compounds with various positively charged terminals (pyridinium and imidazolium derivatives) was synthesized and its gelation behavior in water was investigated. Most of the compounds can be very easily synthesized in high yields (total yields >90%), and they function as excellent hydrogelators that form hydrogels below 1 wt%; particularly, N^{ε}-lauroyl-N^{α}-[11-(4-*tert*-butylpyridinium)undecanoyl]-L-lysine ethyl ester (**2c**) and N^{ε}-lauroyl-N^{α}-[11-(4-phenylpyridinium)undecanoyl]-L-lysine ethyl ester (**2d**), which are able to gel water at concentration of only 0.2 wt%. This corresponds to a gelator molecule that entraps more than 20000 water molecules. All hydrogels are very stable and maintain the gel state for at least 9 months. TEM observations demonstrated that these hydrogelators self-assemble into a nanoscaled fibrous structure; a three-dimensional network is then formed by the entanglement of the nanofibers. An FTIR study in $[D_6]DMSO/D_2O$ and in $CHCl_3$ revealed the existence of intermolecular hydrogen bonding between the amide groups. This was further supported by a ^1H NMR study in $[D_6]DMSO/H_2O$. A luminescence study, in which ANS (1-anilino-8-naphtharenesulfonic acid) was used as a probe, indicated that the hydrogelators self-assemble into nanostructures possessing hydrophobic pockets at a very low concentration. Consequently, it was found that the driving forces for self-assembly into a nanofiber are hydrogel bonding and hydrophobic interactions.

Keywords: gels · hydrogels · self-assembly · supramolecular chemistry

Introduction

Organogels, in which organic solvents are gelled by low-molecular-weight compounds (organogelators), have attracted much interest on account of their unique features and potential applications for new organic soft materials.[1] Many organogelators have been found and their gelation abilities in organic solvents and the physical properties of the organogels have been investigated.[2] Most organogelators self-assemble into nanoscale superstructures, such as fibers, rods, and ribbons, through hydrogen bonding, π-stacking, van der Waals, coordination, and charge-transfer interactions to create three-dimensional networks; this leads to the gelation of organic solvents. Furthermore, organogelators and their organogels have been used for the fabrication of templated materials,[3] sensors,[4] and assemblies with molecular recognition and other properties.[5]

On the other hand, hydrogels have been extensively studied because of their applications for tissue engineering[6] and the development of new materials that reversibly respond to various external stimuli.[7] They usually consist of covalently or noncovalently cross-linked polymers and contain a large amount of water that fills the interstitial spaces in the network. These hydrogels have complicated intermolecular association modes that are difficult to define. In contrast, organogels are one-dimensional aggregates of low-molecular-weight compounds, which leads to a relatively easy definition of the association modes. However, there are only a limited number of hydrogels formed by low-molecular-weight compounds.[8]

One of our challenges is the application of the organogelators as low-molecular-weight *hydrogelators*. On account of their very low solubility or insolubility, it is difficult to dissolve most of the organogelators in water. We focused on the L-lysine derivatives, which are some of the best organogelators based on an amino acid,[2a] and synthesized compound **2a**, which has a positively charged terminal group (Scheme 1). Very interestingly, **2a** is soluble in water on gentle

[a] Dr. M. Suzuki, Prof. Dr. K. Hanabusa
Graduate School of Science and Technology
Shinshu University
Ueda, Nagano 386-8567 (Japan)
Fax: (+81) 268-21-5608
E-mail: msuzuki@giptc.shinshu-u.ac.jp

[b] M. Yumoto, Dr. M. Kimura, Prof. Dr. H. Shirai
Department of Functional Polymer Science
Faculty of Textile Science and Technology
Shinshu University
Ueda, Nagano 386-8567 (Japan)

0947-6539/03/0901-0348 $ 20.00+.50/0 *Chem. Eur. J.* **2003**, *9*, No. 1

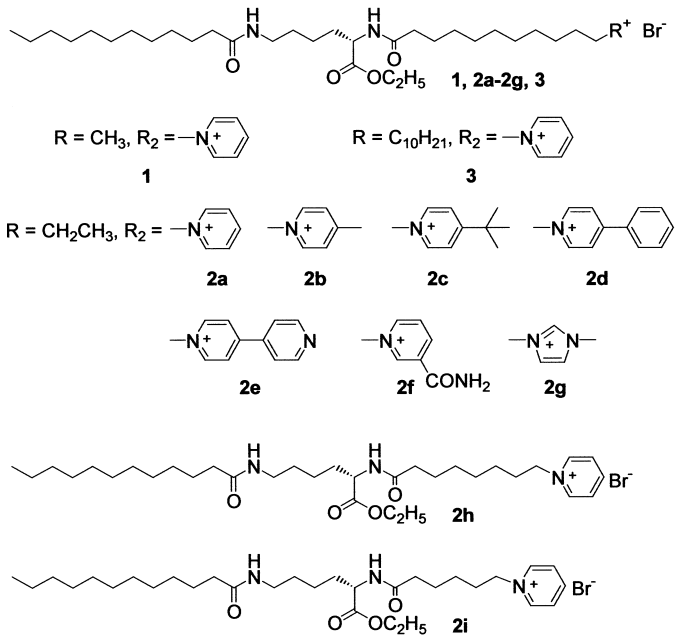

Scheme 1. Chemical structures of low-molecular-weight hydrogelators.

heating (≈40 °C). After allowing the solution to stand at 25 °C, the aqueous solution gelled. In this paper, we describe a family of low-molecular-weight hydrogelators based on L-lysine and their self-assembling behavior as well as its gelation ability in water.

Results and Discussion

Gelation test: When aqueous solutions of **2a**, **2h**, and **2d** were allowed to stand at room temperature, after dissolution of the gelators in water by heating at ≈40 °C, transparent, translucent, and opaque hydrogels formed as shown in Figure 1.

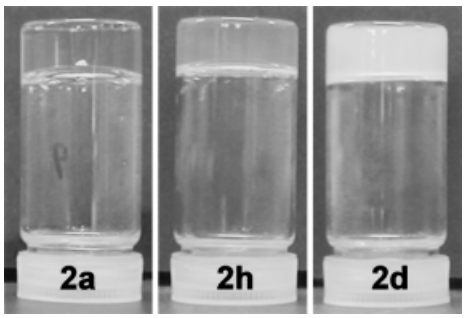

Figure 1. Photographs of hydrogels formed by **2a**, **2h**, and **2d**. [gelator] = 4 mg mL^{-1}.

The gelation test data and the values of the minimum gel concentration (MGC) necessary for the gelation of water are listed in Table 1. Except for **2f** and **2i**, all compounds can gel water below 1 wt %; in particular, **2c** and **2d** form hydrogels at 0.2 wt %, which corresponds to a gelator molecule that entraps more than 20000 water molecules. All hydrogels are very stable and maintain the gel state for at least 9 months. In contrast, **2f** was very soluble in water and did not have any

Table 1. Results of the gelation test for **1**–**3** in water.

	State[a]	MGC [mg mL^{-1}][b]	H_2O/gelator[c]
1	TG	3 (4.5 mM)	12300
2a	TG	3 (4.4 mM)	12500
2b	TG	5 (7.2 mM)	7700
2c	TG	2 (2.7 mM)	20500
2d	OG	2 (2.6 mM)	21000
2e	OG	10 (13.5 mM)	4400
2f	VS	< 2 (2.7 mM)	
	P	≥ 2 (2.7 mM)	
2g	TG	5 (4.5 mM)	7600
2h	TLG	6 (9.4 mM)	5900
2i	S		
3	TLG	6 (9.4 mM)	5930

[a] TG: Transparent gel; TLG: Translucent gel; OG: Opaque gel; VS: Viscous solution; S: Solution (at 5 wt %); P: Precipitation. [b] Values mean minimum gelation concentration necessary for gelation of water [mg mL^{-1}] and its molar concentration. [c] The number of water molecules entrapped by one gelator molecule.

gelation ability for water. However, an interesting result was obtained: the aqueous solution was transparent and highly viscous at 0.2 wt % (2 mg mL^{-1}), while **2f** precipitated above 0.2 wt %. Compound **2f** has an amide group on the pyridine ring that can undergo hydrogen bonding; namely, it has more hydrogen bonding sites than the other compounds. It is probable that **2f** readily crystallizes above 0.2 wt %, because it undergoes stronger hydrogen bonding than the other compounds because of the hydrogen-bonding sites on the pyridine ring.

The gelation significantly depends on the length of the alkyl chains in the ester and the alkylene spacer between the L-lysine segment and the positively charged terminal; the gelation ability decreases with increasing length of the alkyl chain on the ester groups and with the decreasing chain length in the alkylene spacer. The gelation abilities of **1** and **2a** are superior to that of **3**, which contains a longer chain in the ester group, and **2i**, which contains a shorter chain in the alkylene spacer. In fact, **2i** never formed a hydrogel. These results suggest that an appropriate hydrophilic–hydrophobic balance in the gelator molecule is important for the effective gelation of water by the L-lysine derivatives.

Transmission electron microscopy (TEM): Figure 2 shows the TEM images of the samples prepared from **1**, **3**, **2i**, **2a**, **2h**, and **2d** in aqueous solution (Scheme 1).[9] Compounds **1**, **2a**, **2h**, and **2d** self-assemble into nanoscale fibrous structures of ≈15–20 nm for **1** and **2a**, ≈40–100 nm for **2h**, and ≈40–300 nm for **2d**, and create a three-dimensional network structure by entanglement of the self-assembled nanofibers. This fact indicates that the hydrogels are formed by the entrappment of water molecules into the spaces of the three-dimensional networks. Compound **3** self-assembles only into a ribbonlike structure with a width of ≈100–200 nm, but not into a nanofiber. This indicates that intermolecular interactions between the decyl chains tend to favor self-organization into the ribbonlike structure. On the other hand, **2f** also forms self-assembled nanofibers in dilute aqueous solutions; this leads to a highly viscous solution. Addition of further **2f** does not lead to gelation, but to crystallization owing to the strong

  0947-6539/03/0901-0349 $ 20.00+.50/0

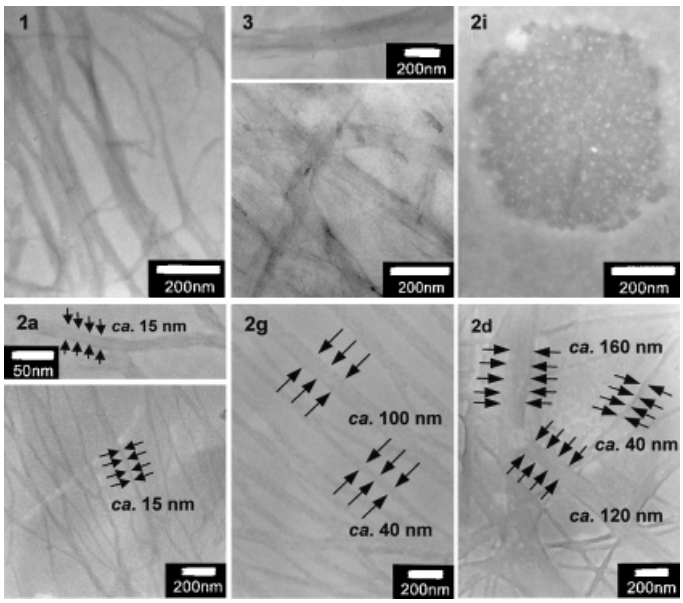

Figure 2. TEM images of samples of **1**, **3**, **2a**, **2d**, **2h**, and **2i** prepared in aqueous solutions with the concentration of MGC for **1**, **3**, **2a**, **2d**, and **2h**, and 10 mM for **2i**.

hydrogen-bonding interaction induced by the amide group on the pyridine ring. As shown in Figure 2, **2i** forms a spherical aggregate that has a diameter of ≈600 nm, but not a nanofiber or a ribbonlike nanostructure; this leads to the nongelation of water.

Very interestingly, the hydrogel state significantly depends on the thickness of the self-assembled nanofibers. The photographs shown in Figure 1 clearly indicate that **2a**, **2h**, and **2d** form transparent, translucent, and opaque hydrogels, respectively.

FTIR spectroscopy: It is well-known that hydrogen bonding is one of the driving forces for the self-assembly of organogelators in organic solvents.[1–2] Although IR spectroscopy is a powerful tool to study hydrogen-bonding interactions, it is very difficult or almost impossible to obtain useful information on the hydrogen-bonding interactions from an FTIR study in H_2O. Therefore, the FTIR spectra were measured in [D_6]DMSO/D_2O. Figure 3 shows the FTIR spectra of **2a** in [D_6]DMSO containing various ratios of D_2O, and the results

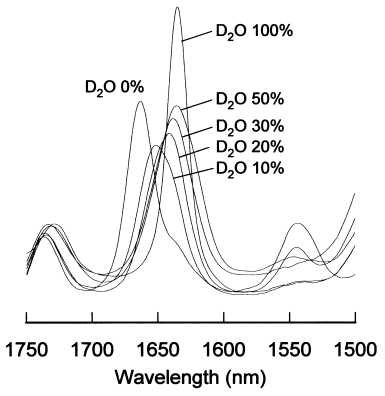

Figure 3. FTIR spectra of hydrogels formed by **2a** in [D_6]DMSO containing various ratios of D_2O.

are listed in Table 2. The FTIR spectrum in [D_6]DMSO, in which no self-assembly occurs, showed absorption bands at 1660 cm^{-1} and 1546 cm^{-1}, which are characteristic of a non-hydrogen-bonding stretching vibration of C=O (amide I) and

Table 2. Absorption frequencies of **2a** in [D_6]DMSO/D_2O.

	ν(C=O) (ester)	ν(C=O) (Amide I)
D_2O 0%	1736	1664
D_2O 10%	1736	1651
D_2O 20%	1735	1641
D_2O 30%	1734	1636
D_2O 50%	1730	1636
D_2O 100%	1728	1635

a hydrogen-bonded bending vibration of N–H (amide II), respectively. In $CHCl_3$, in which no interactions between molecules of **2a** and between molecules of **2a** and solvent molecules occur, a non-hydrogen bonding stretching vibration of C=O (amide I) and a bending vibration of N–H (amide II) appear at 1660 cm^{-1} and 1515 cm^{-1}, respectively. The facts indicate that **2a** undergoes a hydrogen-bonding interaction with DMSO [$(CD_3)_2S{=}O\cdots H{-}N$], but there is no interaction of the amide carbonyl group in **2a**. With increasing D_2O content, the bands of the amide I (νC=O) changed dramatically in two stages: up to a 30% D_2O content, the band shifts from 1660 cm^{-1} to 1635 cm^{-1} with virtually no change in absorbance, and then the absorbance increases above a 30% D_2O content, while and remains at $\nu = 1635\ cm^{-1}$ (no blue shift is observed). In addition, **2a** forms a gel above a 30% D_2O content under the experimental conditions (20 mg mL^{-1}). Such spectral shifts are compatible with the presence of intermolecular hydrogen-bonded amide groups and suggest that one of the driving forces for the hydrogel formation is hydrogen bonding.

The FTIR measurements also provide information on the alkyl groups. The absorption bands of the asymmetric (ν_{as}) and symmetric (ν_s) CH_2 stretching vibrations of **2a** appeared at 2930 cm^{-1} (ν_{as}, C–H) and 2857 cm^{-1} (ν_s, C–H) in $CHCl_3$, while in D_2O they shifted to 2920 cm^{-1} and 2850 cm^{-1}, respectively. Such a low frequency shift is induced by restriction of the alkyl chains in **2a**,[10] thus indicating that the alkyl groups of **2a** strongly organize in the self-assembled nanofibers, presumably through a hydrophobic interaction.

On the other hand, the FTIR spectra of **2i**, which forms a spherical aggregate having diameters of ≈600 nm, also show absorption bands at 1635 cm^{-1} ($\tilde{\nu}$C=O, amide I), indicating that **2i** undergoes an intermolecular hydrogen-bonding interaction in the spherical aggregates. In addition, the absorption bands of ν_{as}C–H and ν_sC–H of **2i** appear at 2925 cm^{-1} and 2850 cm^{-1}, respectively, which are higher frequencies than those of **2a** in D_2O. This fact suggests that the alkyl groups of **2i** in the spherical aggregates are more flexible than those of **2a** in the nanofiber, namely the hydrophobic interaction of **2i** is weaker than that of **2a**.

^{1}H NMR study: To obtain further information on the intermolecular hydrogen bonding interaction between the amide groups, we measured the ^{1}H NMR spectra of **2a** in

0947-6539/03/0901-0350 $ 20.00+.50/0 *Chem. Eur. J.* **2003**, *9*, No. 1

[D_6]DMSO containing various amounts of H_2O.[11] Figure 4 shows the ^{1}H NMR spectra of **2a** in [D_6]DMSO/H_2O, and the chemical shifts of two amide protons are summarized in Table 3. With increasing H_2O content, the chemical shifts of

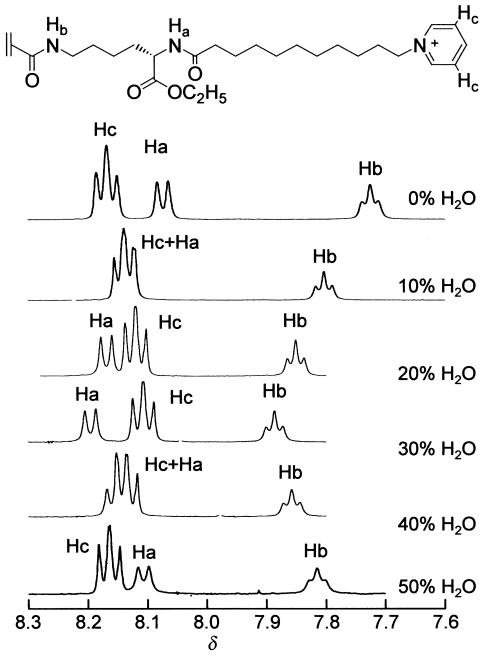

Figure 4. ^{1}H NMR spectra of **2a** in [D_6]DMSO containing various ratios of H_2O.

Table 3. ^{1}H NMR chemical shifts of amide protons of **2a** in [D_6]DMSO/H_2O

	N–H_b	J[Hz]	N–H_a	J[Hz]
H_2O 0%	7.72	5.6	8.07	7.6
H_2O 10%	7.80	5.6	–[a]	–[a]
H_2O 20%	7.85	5.6	8.17	7.6
H_2O 30%	7.89	5.6	8.19	7.6
H_2O 40%	7.86	5.6	–[a]	–[a]
H_2O 50%	7.81	4.8	8.10	6.8

[a] No detection because the peak overlaps with the H_c protons.

the amide protons shift to lower fields for up to 30% additions. Above this level, they then shift upfield. It is generally known that the chemical shifts of amide groups appear further upfield than those undergoing hydrogen bonding with H_2O.[12] Therefore, the changes in the chemical shifts of the amide protons to lower fields for up to a 30% H_2O content and then upfield over 30% reveal that the hydrogen bonding with [D_6]DMSO (–S=O···H–N) replaces that with H_2O (H_2O···H–N), and then with intermolecular hydrogen bonding between the amide groups.

On the other hand, the chemical shift of the pyridinium H_c protons shifted in the opposite direction: it shifted upfield up to a 30% H_2O content, and then into lower field. The addition of water brings about the hydration of the charged pyridinium segments; this leads to the upfield shift. On further addition of water, **2a** molecules self-assemble into the nanofiber and dehydration probably takes place; consequently, the pyridinium H_c protons shift to lower fields.

Luminescence study: To elucidate the self-assembling process, the luminescence spectra were studied with 8-anilino-1-naphthalenesulfonic acid (ANS) as a probe. ANS is one of the popular fluorescence probes for a hydrophobic environment.[13] Figure 5 shows the typical luminescence spectra of

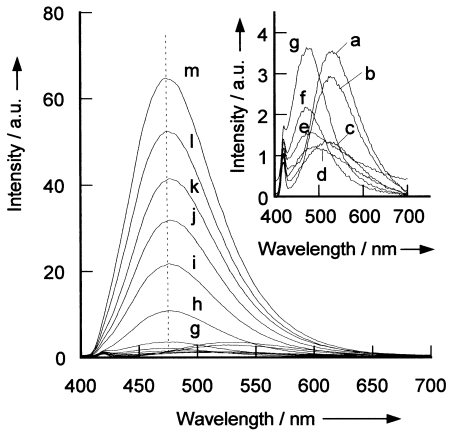

Figure 5. Luminescence spectra of ANS (1.0×10^{-5} M) in aqueous solutions containing various concentrations of **2b**. Where [**2b**]/10^{-4} M: **a**: 0; **b**: 0.1; **c**: 0.5; **d**: 1.0; **e**: 1.5; **f**: 5.0; **g**: 10.0; **h**: 15.0; **i**: 20.0; **j**: 30.0; **k**: 50.0; **l**: 70.0 (MGC); **m**: 100.0.

ANS in aqueous solutions containing various concentrations of **2b**, and Figure 6 shows the dependence of the luminescence maxima (λ_{max}) and the relative luminescence intensities (I/I_0: I_0 and I represent the luminescence intensities of ANS at λ_{max} in the absence and in the presence of **2b** or **2i**, respectively) on the concentration of **2b** and **2i**. Up to 5.0×10^{-4} M of **2b**, the λ_{max} blue-shifts from 534 nm to 469 nm with increasing **2b** concentration. Further addition increases the luminescence intensity, but produces only a slight change in the λ_{max} values. Such luminescence behavior is frequently observed when the ANS molecules are incorporated into a hydrophobic environ-

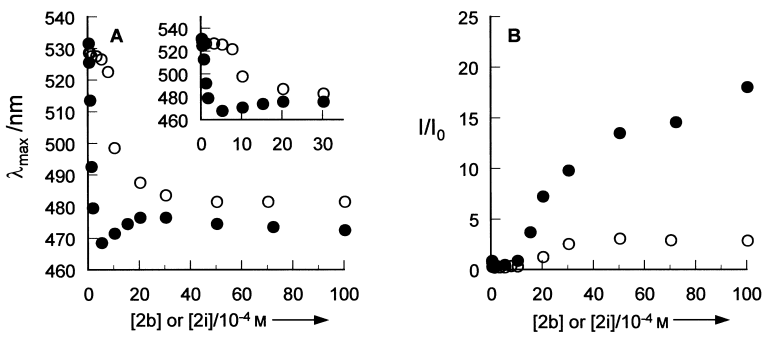

Figure 6. Dependence of the luminescence maxima (λ_{max}) and relative luminescence intensities (I/I_0) on the concentration of **2b** (●) or **2i** (○).

  0947-6539/03/0901-0351 $ 20.00+.50/0

ment; namely, the interior of the strands of self-assembled nanofibers is hydrophobic. Therefore, this result will be prove that one of the driving forces for the self-assembly of **2b** into nanofibers is a hydrophobic interaction, which is supported by the FTIR results in D_2O. In addition, this fact is in agreement with a previous report for amino acid based hydrogelators.[8h]

The luminescence results also suggest that the self-assembly of **2b** into nanofibers proceeds in two steps: for up to 5.0×10^{-4} M, **2b** molecules pre-self-assemble into some aggregates that have hydrophobic pockets (sharp blue-shift and no change in I/I_0), and then they self-assemble into nanofibers (very slight red-shift and increase in I/I_0). In contrast, the luminescence property of ANS in the **2i** system demonstrates a one-step change; the λ_{max} sharply blue-shifts to 489 nm and the luminescence intensity begins to increase at $\approx 1.0 \times 10^{-3}$ M. Similar luminescence behavior is often observed around the critical micelle concentration in various surfactant systems.[14] Therefore, **2i** only self-assembles into a spherical aggregate at $\approx 1.0 \times 10^{-3}$ M.

Compared to **2i**, the λ_{max} values of **2b** appear at a low wavelengths and the luminescence intensity is very high. The luminescence property of ANS is very sensitive to the polarity of its environment; the low polarity brings about a blue-shift in λ_{max} into the lower wavelength and higher intensity.[14a] Considering these facts, the hydrophobicity in the strands of the self-assembled nanofibers of **2b** is higher than that in the spherical aggregate formed by **2i**.

Conclusion

We succeeded in the application of L-lysine-based organogelators as hydrogelators by introduction of a positive charge into the terminal group of the organogelator. These hydrogelators can be synthesized both simply and effectively. In water, the hydrogelators first self-assemble into some aggregates that contain hydrophobic pockets and grow into nanofibers through hydrogen bonding and hydrophobic interactions. The entanglement of the nanofibers forms a three-dimensional network, which leads to hydrogelation.

Experimental Section

Materials: N^{ε}-Lauroyl-L-lysine was obtained from the Ajinomoto. The other chemicals were of the highest grade commercially available and used without further purification. All solvents used in the syntheses were purified, dried, or freshly distilled as required. The N^{ε}-lauroyl-L-lysine ethyl ester (C_2AmiNH_2) was prepared according to the literature.[2a] 11-Bromoundecanoyl chloride and 8-bromooctanoyl chloride were prepared by the reaction of the corresponding acids with thionyl chloride.

Apparatus **for measurements**: Elemental analyses were performed on a Perkin–Elmer series II CHNS/O analyzer 2400. FTIR spectra were recorded on a JASCO FS-420 spectrometer. UV/Vis absorption spectra were acquired on a JASCO V-570 UV/VIS/NIR spectrometer. Luminescence spectra were measured with a JASCO FP-750 spectrofluorometer. TEM images were obtained with a JEOL JEM-2010 electron microscope at 200 kV. ^{1}H NMR spectra were measured on a Bruker AVANCE 400 spectrometer with TMS as the standard.

Gelation test: A mixture of a weighed gelator in water (1 mL) was heated at ≈ 40 °C in a sealed test tube until a clear solution appeared. After allowing the solution to stand at 25 °C for 6 h, the state of the solution was evaluated by the "stable to inversion of a test tube" method.[2a]

Transmission electron microscopy (TEM): Samples were prepared as follows: the aqueous solutions of the gelators were dropped on a collodion- and carbon-coated 400 mesh copper grid and immediately dried in a vacuum for 24 h. After dropping a 2 wt% phosphotungstic acid solution, the grids were dried under reduced pressure for 24 h.

FTIR study: FTIR spectroscopy was performed in $CHCl_3$ (15 mg mL^{-1} of gelators) and in [D$_6$]DMSO/D_2O (20 mg mL^{-1} of gelators) operating at a 2 cm^{-1} resolution with 32 scans. The spectroscopic cell with a CaF_2 window and 25 μm spacers in [D$_6$]DMSO/D_2O or 200 μm spacers in $CHCl_3$ was used for the measurements.

^{1}H NMR study: Solutions of **2a** (20 mg mL^{-1}) were prepared in [D$_6$]DMSO containing various ratios of H_2O, namely, 0%, 10%, 20%, 30%, 40%, and 50%.

Fluorescence study: Fluorescence spectra were measured at [ANS] $= 1.0 \times 10^{-5}$ M and [gelator] $= 0$–10 mM in a fluorescence spectroscopic cell (1 cm × 1 cm). The excitation wavelength was 356 nm, corresponding to the absorption maximum.

***N*$^{\varepsilon}$-Lauroyl-L-lysine methyl ester (C_1AmiNH_2)**: A suspension of N^{ε}-Lauroyl-L-lysine (0.33 mol) in methanol (800 mL) was saturated with dry HCl in an ice bath. After standing overnight at room temperature, excess HCl and methanol were completely removed by evaporation. THF (400 mL) was added to the residue, and the solution was allowed to stand in a refrigerator for 6 h. The resulting white precipitate was filtered, washed with diethyl ether, and then dried. The HCl salt of C_1AmiNH_2 was dissolved in water (2 L), and a large excess of morpholine (2.3 mol) was added with vigorous stirring. The white precipitate was collected by filtration, washed with water, and then dried. C_1AmiNH_2 was purified by recrystallization from ligroin (96%). M.p. 72–74 °C; IR (KBr): $\tilde{\nu} = 3389$ (N–H, amine), 3332 (N–H, amide A), 1726 (C=O, ester), 1642 (C=O, amide I), 1544 cm^{-1} (δN–H, amide II); elemental analysis calcd (%) for $C_{19}H_{38}N_2O_3$ (342.52): C 66.63, H 11.18, N 8.18; found: C 66.63, H 11.24, N 8.08.

***N*$^{\varepsilon}$-Lauroyl-L-lysine decyl ester ($C_{10}AmiNH_2$)**: A mixture of N^{ε}-Lauroyl-L-lysine (0.16 mol), 1-decanol (0.29 mol), and *p*-toluenesulfonic acid monohydrate (0.33 mol) in Benzene (400 mL) was refluxed at 130 °C for 48 h, while removing water. The excess benzene was evaporated, and diethyl ether was added. After allowing the solution to stand in a refrigerator for 12 h, the *p*-toluenesulfonic acid salt of $C_{10}AmiNH_2$ was filtered and washed with diethyl ether. The solid was dissolved in methanol (250 mL), and a large excess of morpholine (0.80 mol) was added with stirring. After the addition of water to the resulting solution, the white precipitate was filtered, washed with water, and dried. $C_{10}AmiNH_2$ was purified by recrystallization from ligroin (93%). M.p. 76–78 °C; IR (KBr): $\tilde{\nu} = 3390$ (N–H, amine), 3333 (N–H, amide A), 1724 (C=O, ester), 1643 (C=O, amide I), 1543 cm^{-1} (δN–H, amide II); elemental analysis calcd (%) for $C_{28}H_{56}N_2O_3$ (486.76): C 71.74, H 12.04, N 5.98; found: C 71.93, H 12.55, N 6.07.

***N*$^{\varepsilon}$-(11-Bromoundecanoyl)-*N*$^{\varepsilon}$-lauroyl-L-lysine methyl ester ($C_1AmiC_{11}Br$)**: 11-Bromoundecanoyl chloride (13.0 mmol) was slowly added to a dry THF solution (100 mL) of the C_1AmiNH_2 (11.6 mmol) and triethylamine (60.0 mmol) at 0 °C with stirring. The resulting solution was stirred at room temperature for 24 h. Then it was reheated to 60 °C and was filtered hot; the filtrate was evaporated to dryness. The crude product was purified by two recrystallizations from ethyl acetate/diethyl ether (97%). M.p. 100–102 °C; ^{1}H NMR (400 MHz, $CDCl_3$, TMS, 25 °C): $\delta = 0.88$ (t, $J = 6.8$ Hz, 3H; CH_3), 3.27–3.21 (m, 2H; CONHCH_2), 3.4 (t, 2H; CH_2Br), 3.74 (s, 3H; OCH_3), 4.55–4.60 (m 1H; CONHC*H*), 5.7 (t, $J = 5.1$ Hz, 1H; CON*H*,), 6.2 ppm (d, $J = 7.8$ Hz, 1H; CON*H*,); IR (KBr): $\tilde{\nu} = 3304$ (N–H, amide A), 1737 (C=O, ester), 1643 (C=O, amide I), 1545 cm^{-1} (δN–H, amide II); elemental analysis calcd (%) for $C_{30}H_{57}N_2O_4Br$ (589.77): C 61.09, H 9.76, N 4.75; found: C 60.94, H 10.11, N 4.81.

***N*$^{\varepsilon}$-(11-Bromoundecanoyl)-*N*$^{\varepsilon}$-lauroyl-L-lysine ethyl ester ($C_2AmiC_{11}Br$)**: The same procedure as for $C_1AmiC_{11}Br$ was used. Yield: 96%; m.p. 101–103 °C; ^{1}H NMR (400 MHz, $CDCl_3$, TMS): $\delta = 0.87$ (t, $J = 6.9$ Hz, 3H; CH_3), 3.23 (q, $J = 6.2$ Hz, 2H; CONHCH_2), 3.40 (t, $J = 6.8$ Hz, 2H; CH_2Br), 4.19 (q, $J = 7.1$ Hz, 2H; OCH_2), 4.52–4.57 (m, 1H, CONHC*H*), 5.76 (t, $J = 5.3$ Hz, 1H; CON*H*), 6.21 ppm (d, $J = 7.8$ Hz, 1H; CON*H*); IR (KBr): $\tilde{\nu} = 3310$ (N–H, amide A), 1732 (C=O, ester), 1643 (C=O, amide I), 1544 cm^{-1}

0947-6539/03/0901-0352 $ 20.00+.50/0 *Chem. Eur. J.* **2003**, *9*, No. 1

(δN–H, amide II); elemental analysis calcd (%) for $C_{31}H_{59}N_2O_4Br$ (603.80): C 61.66, H 9.87, N 4.64; found: C 61.74, H 10.07, N 4.66.

N^{α}-(11-Bromoundecanoyl)-N^{ε}-lauroyl-L-lysine decyl ester ($C_{10}AmiC_{11}Br$): The same procedure as for $C_1AmiC_{11}Br$ was used. Yield: 88%; m.p. 99–101 °C; IR (KBr): $\tilde{\nu}$ = 3305 (N–H, amide A), 1732 (C=O, ester), 1643 (C=O, amide I), 1539 cm^{-1} (δN–H, amide II); elemental analysis calcd (%) for $C_{39}H_{75}N_2O_4Br$ (715.93): C 65.43, H 10.56, N 3.91; found: C 65.54, H 10.99, N 3.97.

N^{α}-(8-Bromooctanoyl)-N^{ε}-lauroyl-L-lysine ethyl ester (C_2AmiC_8Br): The same procedure as for $C_1AmiC_{11}Br$ was used but with 8-bromooctanoyl chloride. Yield: 95%; m.p. 94–96 °C; IR (KBr): $\tilde{\nu}$ = 3310 (N–H, amide A), 1740 (C=O, ester), 1641 (C=O, amide I), 1546 cm^{-1} (δN–H, amide II); elemental analysis calcd (%) for $C_{28}H_{53}N_2O_4Br$ (561.64): C 59.88, H 9.51, N 4.99; found: C 60.12, H 9.84, N 5.02.

N^{α}-(6-Bromohexanoyl)-N^{ε}-lauroyl-L-lysine ethyl ester (C_2AmiC_6Br): The same procedure as for $C_1AmiC_{11}Br$ was used but with 6-bromohexanoyl chloride. Yield: 97%; m.p. 93–95 °C; IR (KBr): $\tilde{\nu}$ = 3310 (N–H, amide A), 1732 (C=O, ester), 1643 (C=O, amide I), 1544 cm^{-1} (δN–H, amide II); elemental analysis calcd (%) for $C_{26}H_{49}N_2O_4Br$ (533.65): C 58.52, H 9.26, N 5.25; found: C 58.77, H 9.44, N 5.34.

N^{α}-(11-Pyridiniumundecanoyl)-N^{ε}-lauroyl-L-lysine methyl ester bromide (1): A solution of $C_1AmiC_{11}Br$ (8.3 mmol) and pyridine (150 mL) in dry DMF (20 mL) was heated at 100 °C for 48 h under a nitrogen atmosphere. The resulting solution was evaporated to dryness. The product was obtained by two recrystallizations from ethyl acetate/diethyl ether (98%). M.p. 93–95 °C; IR (KBr): $\tilde{\nu}$ = 3316 (N–H, amide A), 1737 (C=O, ester), 1638 (C=O, amide I), 1543 cm^{-1} (δN–H, amide II); elemental analysis calcd (%) for $C_{35}H_{62}N_3O_4Br$ (668.79): C 62.86, H 9.34, N 6.28; found: C 63.01, H 9.55, N 6.34.

N^{α}-(11-Pyridiniumundecanoyl)-N^{ε}-lauroyl-L-lysine decyl ester bromide (3): The same procedure as for **1** was used but with $C_{10}AmiNH_2$. Yield: 93%; m.p. 89–91 °C; ^{1}H NMR (400 MHz, $CDCl_3$, TMS): δ = 0.88 (t, J = 6.8 Hz, 6H; CH_3), 3.23 (q, J = 6.6 Hz, 2H; CONHCH_2), 4.10 (t, J = 6.4 Hz, 2H; OCH_2), 4.47–4.52 (m, 1H; CONHC*H*), 5.01 (t, J = 7.4 Hz, 2H; CH_2Py), 6.24 (t, J = 5.6 Hz, 1H; CON*H*), 6.64 (d, J = 7.6 Hz, 1H; CON*H*), 8.15 (t, J = 7.4 Hz, 2H; 3-Py*H*), 8.52 (t, J = 7.8 Hz, 1H; 4-Py*H*), 9.54 ppm (d, J = 5.6 Hz, 2H, 2-Py*H*); IR (KBr): $\tilde{\nu}$ = 3298 (N–H, amide A), 1737 (C=O, ester), 1642 (C=O, amide I), 1538 cm^{-1} (δN–H, amide II); elemental analysis calcd (%) for $C_{44}H_{80}N_3O_4Br$ (795.03): C 66.47, H 10.14, N 5.29; found: C 66.57, H 10.55, N 5.26.

N^{α}-(11-Pyridiniumundecanoyl)-N^{ε}-lauroyl-L-lysine ethyl ester bromide (2a): The same procedure as for **1** was used but with C_2AmiNH_2. Yield: 93%; m.p. 93–95 °C; ^{1}H NMR (400 MHz, $CDCl_3$, TMS): δ = 0.87 (t, J = 6.8 Hz, 3H; CH_3), 3.22 (q, J = 6.6 Hz, 2H; CONHCH_2), 4.16 (q, J = 7.2 Hz, 2H; OCH_2), 4.45–4.49 (m 1H; CONHC*H*), 5.00 (t, J = 7.4 Hz, 2H; CH_2Py), 6.39 (t, J = 5.5 Hz, 1H; CON*H*), 6.78 (d, J = 7.4 Hz, 1H; CON*H*), 8.17 (t, J = 7.2 Hz, 2H; 3-Py*H*), 8.54 (t, J = 7.8 Hz, 1H; 4-Py*H*), 9.57 ppm (d, J = 5.6 Hz, 2H; 2-Py*H*); IR (KBr): $\tilde{\nu}$ = 3309 (N–H, amide A), 1727 (C=O, ester), 1640 (C=O, amide I), 1543 cm^{-1} (δN–H, amide II); elemental analysis calcd (%) for $C_{36}H_{64}N_3O_4Br$ (682.82): C 63.32, H 9.45, N 6.15; found: C 63.45, H 9.75, N 6.18.

N^{α}-[11-(4-Methylpyridinium)undecanoyl]-N^{ε}-lauroyl-L-lysine ethyl ester bromide (2b): The same procedure as for **2a** was used but with 4-methylpyridine. Yield: 95%; m.p. 74–76 °C; ^{1}H NMR (400 MHz, $CDCl_3$, TMS): δ = 0.87 (t, J = 6.8 Hz, 3H; CH_3), 3.22 (q, J = 6.7 Hz, 2H; CONHCH_2), 4.17 (q, J = 7.1 Hz, 2H; OCH_2), 4.45–4.50 (m, 1H; CONHC*H*), 4.89 (t, J = 7.4 Hz, 2H; CH_2MePy), 6.34 (t, J = 5.5 Hz, 1H; CON*H*), 6.71 (d, J = 7.3 Hz, 1H; CON*H*), 7.89 (d, J = 6.3 Hz, 2H; 3-MePy*H*), 9.32 ppm (d, J = 6.8 Hz, 2H; 2-Py*H*); IR (KBr): $\tilde{\nu}$ = 3308 (N–H, amide A), 1735 (C=O, ester), 1640 (C=O, amide I), 1544 cm^{-1} (δN–H, amide II); elemental analysis calcd (%) for $C_{37}H_{66}N_3O_4Br$ (696.84): C 63.77, H 9.55, N 6.03; found: C 63.88, H 9.75, N 5.99.

N^{α}-[11-(4-*tert*-Butylpyridinium)undecanoyl]-N^{ε}-lauroyl-L-lysine ethyl ester bromide (2c): The same procedure as for **2a** was used but with 4-*tert*-butylpyridine. Yield: 92%; m.p. 57–59 °C; ^{1}H NMR (400 MHz, $CDCl_3$, TMS): δ = 0.88 (t, J = 6.8 Hz, 3H; CH_3), 3.23 (q, J = 6.5 Hz, 2H; CONHCH_2), 4.17 (q, J = 7.1 Hz, 2H; OCH_2), 4.48–4.53 (m, 1H; CONHC*H*), 4.92 (t, J = 7.4 Hz, 2H; CH_2BuPy), 6.25 (t, J = 5.6 Hz, 1H; CON*H*), 6.62 (d, J = 7.6 Hz, 1H; CON*H*), 8.00 (d, J = 6.8 Hz, 2H; 3-BuPy*H*), 9.42 ppm (d, J = 6.8 Hz, 2H; 2-BuPy*H*); IR (KBr): $\tilde{\nu}$ = 3310 (N–H, amide A), 1727 (C=O, ester), 1639 (C=O, amide I), 1545 cm^{-1} (δN–H, amide II); elemental analysis calcd (%) for $C_{40}H_{72}N_3O_4Br$ (738.92): C 65.02, H 9.82, N 5.69; found: C 65.12, H 10.14, N 5.74.

N^{α}-[11-(4-Phenylpyridinium)undecanoyl]-N^{ε}-lauroyl-L-lysine ethyl ester bromide (2d): The same procedure as for **2a** was used but with 4-phenylpyridine. Yield: 97%; m.p. 81–83 °C; ^{1}H NMR (400 MHz, $CDCl_3$, TMS): δ = 0.87 (t, J = 6.8 Hz, 3H; CH_3), 3.22 (q, J = 6.2 Hz, 2H; CONHCH_2), 4.16 (q, J = 7.0 Hz, 2H; OCH_2), 4.45–4.50 (m, 1H; CONHC*H*), 4.93 (t, J = 7.4 Hz, 2H; CH_2PhPy), 6.44 (t, J = 5.6 Hz, 1H; CON*H*), 6.80 (d, J = 7.6 Hz, 1H; CON*H*), 7.56–7.64 (m, 3H; 7-PhPy*H*, 8-PhPy*H*), 7.83 (d, J = 6.3 Hz, 2H; 6-PhPy*H*), 8.29 (d, J = 6.8 Hz, 2H; 3-PhPy*H*), 9.52 ppm (d, J = 6.8 Hz, 2H; 2-PhPy*H*); IR (KBr): $\tilde{\nu}$ = 3310 (N–H, amide A), 1735 (C=O, ester), 1640 (C=O, amide I), 1548 cm^{-1} (δN–H, amide II); elemental analysis calcd (%) for $C_{42}H_{68}N_3O_4Br$ (758.91): C 66.47, H 9.03, N 5.54; found: C 66.54, H 9.44, N 5.64.

N^{α}-[11-(4-(4′-Pyridyl)pyridinium)undecanoyl]-N^{ε}-lauroyl-L-lysine ethyl ester bromide (2e): $C_2AmiC_{11}Br$ (8.3 mmol) and 4,4′-bipyridine (8.5 mmol) were refluxed in dry acetonitrile (600 mL) for 24 h. After cooling to room temperature, the yellow insoluble compound was filtered off. The filtrate was evaporated to dryness. The product was obtained by two recrystallizations from ethyl acetate/diethyl ether. Yield: 80%; m.p. 84–86 °C; ^{1}H NMR (400 MHz, $CDCl_3$, TMS): δ = 0.87 (t, J = 6.8 Hz, 3H; CH_3), 3.22 (q, J = 6.5 Hz, 2H; CONHCH_2), 4.16 (q, J = 7.1 Hz, 2H; OCH_2), 4.44–4.49 (m, 1H; CONHC*H*), 5.01 (t, J = 7.4 Hz, 2H; CH_2Bpy), 6.32 (t, J = 5.6 Hz, 1H; CON*H*), 6.80 (d, J = 7.3 Hz, 1H; CON*H*), 7.77 (d, J = 6.0 Hz, 2H; 2′-Bpy*H*), 8.46 (d, J = 7.1 Hz, 2H; 3-Bpy*H*), 8.88 (d, J = 6.0 Hz, 2H; 1′-Bpy*H*), 9.68 ppm (d, J = 6.8 Hz, 2H; 2-Bpy*H*); IR (KBr): $\tilde{\nu}$ = 3309 (N–H, amide A), 1733 (C=O, ester), 1640 (C=O, amide I), 1543 cm^{-1} (δN–H, amide II); elemental analysis calcd (%) for $C_{41}H_{67}N_4O_4Br$ (759.90): C 64.79, H 8.90, N 7.36; found: C 64.98, H 9.14, N 7.44.

N^{α}-[11-(3-Aminocarbonylpyridinium)undecanoyl]-N^{ε}-lauroyl-L-lysine ethyl ester bromide (2f): The same procedure as for **2a** was used but with nicotinamide. Yield: 89%; m.p. 152–154 °C; IR (KBr): $\tilde{\nu}$ = 3313 (N–H, amide A), 3156 (N–H, NH_2 amide), 1731 (C=O, ester), 1701 (C=O, amide), 1640 (C=O, amide I), 1544 cm^{-1} (δN–H, amide II); elemental analysis calcd (%) for $C_{37}H_{65}N_4O_5Br$ (725.84): C 61.23, H 9.03, N 7.72; found: C 61.44, H 9.24, N 7.72.

N^{α}-[11-(1-Methylimidazolium)undecanoyl]-N^{ε}-lauroyl-L-lysine ethyl ester bromide (2g): The same procedure as for **2a** was used but with 1-methylimidazole. Yield: 95%; m.p. 80–82 °C; ^{1}H NMR (400 MHz, $CDCl_3$, TMS): δ = 0.88 (t, J = 6.7 Hz, 3H; CH_3), 3.22 (q, J = 6.3 Hz, 2H; CONHCH_2), 4.12 (s, 1H; MeImCH_3), 4.17 (q, J = 7.1 Hz, 2H; OCH_2), 4.32 (t, J = 7.4 Hz, 2H; CH2MeIm), 4.48 (br, 1H; CONHC*H*), 6.31 (br, 1H; CON*H*), 6.79 (br, 1H; CON*H*) 7.43 (br, 1H; 4-MeIm*H*), 7.49 (br, 1H; 5-MeIm*H*), 10.42 ppm (s, 1H; 2MeIm*H*); IR (KBr): $\tilde{\nu}$ = 3312 (N–H, amide A), 1736 (C=O, ester), 1639 (C=O, amide I), 1544 cm^{-1} (δN–H, amide II); elemental analysis calcd (%) for $C_{35}H_{65}N_4O_4Br$ (685.82): C 61.28, H 9.57, N 8.17; found: C 61.33, H 9.66, N 8.24.

N^{α}-[8-Pyridiniumoctanoyl]-N^{ε}-lauroyl-L-lysine ethyl ester bromide (2h): The same procedure as for **2a** was used but with C_2AmiC_8Br. Yield: 97%; m.p. 92–94 °C; ^{1}H NMR (400 MHz, $CDCl_3$, TMS): δ = 0.87 (t, J = 6.8 Hz, 3H; CH_3), 3.15–3.28 (m, 2H; CONHCH_2), 4.14 (q, J = 7.1 Hz, 2H; OCH_2), 4.43 (q, J = 6.8 Hz, 1H; CONHC*H*), 4.49–5.08 (m, 2H; CH_2Py), 6.60 (t, J = 5.6 Hz, 1H; CON*H*), 7.28 (d, J = 7.8 Hz, 1H; CON*H*), 8.13 (t, J = 7.2 Hz, 2H; 3-Py*H*), 8.51 (t, J = 7.8 Hz, 1H; 4-Py*H*), 9.57 ppm (d, J = 5.6 Hz, 2H; 2-Py*H*); IR (KBr): 3310 (N–H, amide A), 1726 (C=O, ester), 1640 (C=O, amide I), 1544 cm^{-1} (δN–H, amide II); elemental analysis calcd (%) for $C_{33}H_{58}N_3O_4Br$ (640.74): C 61.86, H 9.12, N 6.56; found: C 61.99, H 9.34, N 6.61.

N^{α}-[6-Pyridiniumhexanoyl]-N^{ε}-lauroyl-L-lysine ethyl ester bromide (2i): The same procedure as for **2a** was used but with C_2AmiC_6Br. Yield: 97%; m.p. 88–9 °C; ^{1}H NMR (400 MHz, $CDCl_3$, TMS): δ = 0.87 (t, J = 6.8 Hz, 3H; CH_3), 3.14–3.32 (m, 2H; CONHCH_2), 4.08–4.16 (m, 2H; OCH_2), 4.35–4.39 (m, 1H; CONHC*H*), 4.91–4.96 (m, 2H; CH_2Py), 6.76 (t, J = 5.5 Hz, 1H; CON*H*), 7.73 (d, J = 7.4 Hz, 1H; CON*H*), 8.11 (t, J = 7.2 Hz, 2H; 3-Py*H*), 8.50 (t, J = 7.8 Hz, 1H; 4-Py*H*), 9.56 ppm (d, J = 5.6 Hz, 2H; 2-Py*H*); IR (KBr): $\tilde{\nu}$ = 3318 (N–H, amide A), 1728 (C=O, ester), 1642 (C=O, amide I), 1540 cm^{-1} (δN–H, amide II); elemental analysis calcd (%) for $C_{31}H_{54}N_3O_4Br$ (612.68): C 60.77, H 8.88, N 6.86; found: C 60.84, H 9.14, N 6.93.

Acknowledgement

This study was supported by a Grant-in-Aid for COE Research (10CE2003), a Grant-in-Aid for Scientific Research on Priority Areas (A), "Dynamic Control of Strongly Correlated Soft Materials" (No. 413/13031036) from the Ministry of Education, Sports, Culture, Science, and Technology of Japan, and The Kao Foundation for Arts and Science.

[1] For excellent reviews see: a) P. Terech, R. G. Weiss, *Chem. Rev.* **1997**, *97*, 3133 – 3159; b) P. Terech, *Ber. Bunsenges. Phys. Chem.* **1998**, *102*, 1630 – 1643; c) J. H. van Esch, B. L. Feringa, *Angew. Chem.* **2000**, *112*, 2351 – 2354; *Angew. Chem. Int. Ed.* **2000**, *39*, 2263 – 2266; d) D. J. Abdallah, R. G. Weiss, *Adv. Mater.* **2000**, *12*, 1237 – 1247.

[2] For recent literature see: a) K. Hanabusa, H. Nakayama, M. Kimura, H. Shirai, *Chem. Lett.* **2000**, 1070 – 1071; b) D. J. Abdallah, S. A. Sirchio, R. G. Weiss, *Langmuir* **2000**, *16*, 7558 – 7561; c) J. H. Jung, Y. Ono, K. Hanabusa, S. Shinkai, *J. Am. Chem. Soc.* **2000**, *122*, 5008 – 5009; d) M. de Loos, J. van Esch, R. M. Kellogg, B. L. Feringa, *Angew. Chem.* **2001**, *113*, 633 – 636; *Angew. Chem. Int. Ed.* **2001**, *40*, 613 – 616; e) H. M. Willemen, T. Vermonden, A. T. M. Marcelis, E. J. R. Sudhölter, *Eur. J. Org. Chem.* **2001**, 2329 – 2335; f) K. S. Partridge, D. K. Smith, G. M. Dykes, P. T. McGrail, *Chem. Commun.* **2001**, 319 – 320; g) R. P. Lyon, W. M. Atkins, *J. Am. Chem. Soc.* **2001**, *123*, 4408 – 4413; h) A. Ajayaghosh, S. J. George, *J. Am. Chem. Soc.* **2001**, *123*, 5148 – 5149; i) E. Snip, S. Shinkai, D. N. Reinhoudt, *Tetrahedron Lett.* **2001**, *42*, 2153 – 5156.

[3] a) W. Gu, L. Lu, G. B. Chapman, R. G. Weiss, *Chem. Commun.* **1997**, 543 – 544; b) R. J. H. Hafkamp, B. P. A. Kokke, I. M. Danke, H. P. M. Geurts, A. E. Rowan, M. C. Feiters, R. J. M. Nolte, *Chem. Commun.* **1997**, 545 – 546; c) S. Kobayashi, K. Hanabusa, N. Hamasaki, M. Kimura, H. Shirai, S. Shinkai, *Chem. Mater.* **2000**, *12*, 1523 – 1525; d) J. H. Jung, H. Kobayashi, M. Masuda, T. Shimizu, S. Shinkai, *J. Am. Chem. Soc.* **2001**, *123*, 8785 – 8789.

[4] a) S. Li, V. T. John, G. C. Irvin, S. H. Bachakonda, G. L. Mcpherson, C. J. O'Connor, *J. Appl. Phys.* **1999**, *85*, 5965 – 5967; b) N. Velasco-Garcia, M. J. Valencia-Gonzàes, M. E. Diaz-Garcia, *Analyst* **1997**, *122*, 5008 – 5009.

[5] a) K. Hanabusa, K. Hiratsuka, M. Kimura, H. Shirai, *Chem. Mater.* **1999**, *11*, 649 – 656; b) N. Mizoshita, K. Kutsuna, K. Hanabusa, T. Kato, *J. Photopolym. Sci. Technol.* **2000**, *13*, 307 – 313; c) L. Gu, Y. Zhao, *Chem. Mater.* **2000**, *12*, 3667 – 3673; d) F. Placin, J.-P. Desvergne, J.-C. Lasségus, *Chem. Mater.* **2001**, *13*, 117 – 131; e) W. Kubo, K. Murakoshi, T. Kitamura, S. Yoshida, K. Hanabusa, H. Shirai, Y. Wada, S. Yanagida, *J. Phys. Chem. B* **2001**, *105*, 12809 – 12815; f) W. Kubo, T. Kitamura, K. Hanabusa, Y. Wada, S. Yanagida, *Chem. Commun.* **2002**, 374 – 375.

[6] K. Yong, D. J. Mooney, *Chem. Rev.* **2001**, *101*, 1869 – 1880.

[7] a) B. Zhao, J. S. Moore, *Langmuir* **2001**, *17*, 4758 – 4763; b) Y. Luo, P. D. Dalton, M. S. Shoichet, *Chem. Mater.* **2001**, *13*, 4087 – 4093; c) V. Pardo-Yissar, R. Gabai, A. N. Shipway, T. Bourenko, I. Willner, *Adv. Mater.* **2001**, *13*, 1320 – 1323; d) Z. Hu, X. Lu, J. Gao, *Adv. Mater.* **2001**, *13*, 1708 – 1712.

[8] a) S. Bhattacharya, S. N. G. Acharya, *Chem. Mater.* **1999**, *11*, 3504 – 3511; b) L. A. Estroff, A. D. Hamilton, *Angew. Chem.* **2001**, *113*, 3589 – 3592; *Angew. Chem. Int. Ed.* **2001**, *39*, 3447 – 3450; c) S. Bhattacharya, S. N. G. Acharya, *Langmuir* **2000**, *16*, 87 – 97; d) F. M. Menger, K. L. Caran, *J. Am. Chem. Soc.* **2000**, *122*, 11679 – 11691; e) U. Maitra, S. Mukhopadhyay, A. Sarkar, P. Rao, S. S. Indi, *Angew. Chem.* **2001**, *113*, 2341 – 2343; *Angew. Chem. Int. Ed.* **2001**, *40*, 2281 – 2283; f) M. Amaike, H. Kobayashi, S. Shinkai, *Chem. Lett.* **2001**, 620 – 621; g) J.-H. Jung, G. John, M. Masuda, K. Yoshida, S. Shinkai, T. Shimizu, *Langmuir* **2001**, *17*, 7229 – 7232; h) J. Makarević, M. Kokić, B. Perić, V. Tomišić, B. Kojić-Prodić, M. Žinić, *Chem. Eur. J.* **2001**, *7*, 3328 – 3341; i) B. A. Simmons, G. C. Irvin, V. Agarwal, A. Rose, V. T. John, G. L. McPherson, N. P. Balsara, *Langmuir* **2002**, *18*, 624 – 632; j) M. Suzuki, M. Yumoto, M. Kimura, H. Shirai, K. Hanabusa, *Chem. Commun.* **2002**, 884 – 885; k) M. Suzuki, M. Yumoto, M. Kimura, H. Shirai, K. Hanabusa, *New J. Chem.* **2002**, *26*, 817 – 818.

[9] Samples were prepared from 0.1 wt % aqueous solutions.

[10] a) N. Yamada, T. Imai, E. Koyama, *Langmuir* **2001**, *17*, 961 – 963; b) X. Wang, Y. Shen, Y. Pan, Y. Liang, *Langmuir* **2001**, *17*, 3162 – 3167.

[11] It is generally known that the amide protons (N–H) in D_2O do not appear in the ^1H NMR spectrum because of H/D exchange. In fact, the amide protons were not observed in [D_6]DMSO/D_2O. Moreover, the ^1H NMR spectrum measurements could not be performed in [D_6]DMSO containing over 50 % H_2O content on account of complete gelation. Therefore, the ^1H NMR study was carried out in [D_6]DMSO/H_2O (H_2O content up to 50 %).

[12] F. H. Billiot, M. McCarroll, E. J. Billiot, J. K. Rugutt, K. Morris, I. M. Warner, *Langmuir* **2002**, *18*, 2993 – 2997.

[13] a) L. Stryer, *Science* **1968**, *162*, 526 – 533; b) R. P. DeToma, J. H. Easter, L. Brand, *J. Am. Chem. Soc.* **1976**, *98*, 5001 – 5007.

[14] J. H. Mathias, M. J. Rosen, L. Davenport, *Langmuir* **2001**, *17*, 6148 – 6154.

Received: August 29, 2002 [F4378]

